Inorganic Chemistry, Vol. 15, No. 8, 1976 **1861**

Contribution from the Department of Chemistry,
Texas A&M University, College Station, Texas 77843

Bonding Implications of the Resistance of Dimolybdenum(II) to Attach Axial Ligands. Structures of Two Polypyrazolylborate Complexes

DOUGLAS M. COLLINS, F. ALBERT COTTON,* and CARLOS A. MURILLO

Received February 24, 1976 AIC601479

Tetrakis(diethyldipyrazolylborato)dimolybdenum (**1**), diacetato(diethyldipyrazolylborato)dimolybdenum (**2**), and diacetatobis(tripyrazolylborato)dimolybdenum (**3**) have been prepared. The structures of the last two have been determined by x-ray crystallography. The Mo–Mo distance in **3** (2.147 (3) Å), where there is a weakly bonded axial ligand on one of the molybdenum atoms, is longer than that in **2** (2.129 (1) Å), where there is no such intramolecular coordination. Possible reasons for the small tendency to bind axial ligands by species containing multiple bonds, as reflected in the above structures, are discussed. The crystallographic data for $Mo_2((pz)_2BEt_2)_2(OOCCH_3)_2 \cdot CS_2$ (pz = 1-pyrazolyl, Et = ethyl) are space group $P\bar{1}$, a = 12.933 (4) Å, b = 13.088 (4) Å, c = 11.592 (4) Å, α = 101.68 (3)°, β = 112.86 (3)°, γ = 69.69 (2)°, V = 1690 (1) Å^3, and Z = 2, and those for $Mo_2((pz)_3BH)_2(OOCCH_3)_2$ are space group $P2_1$, a = 11.238 (8) Å, b = 13.698 (6) Å, c = 9.681 (7) Å, β = 99.34 (6)°, V = 1471 (2) Å^3, and Z = 2.

Introduction

It is now well established[1] by experimental data that species containing multiple metal–metal bonds show little—or at best only a moderate—tendency to bind ligands in the axial positions, that is, in positions opposite (trans) to the M–M multiple bond. Thus many compounds such as $Mo_2(O_2CR)_4$ species, $Mo_2(CH_3)_8^{4-}$, $Mo_2Cl_8^{4-}$, $Cr_2(CH_3)_8^{4-}$, $Tc_2Cl_8^{3-}$, $Re_2Cl_8^{2-}$, and $Re_2Br_8^{2-}$ are obtained in crystalline compounds without the presence of any axial ligands even when the crystals are deposited from solutions containing potential ligands such as H_2O, ROH, or THF. In some cases, when very good ligands are available (e.g., pyridine, Cl^-), compounds are obtained in which these are weakly coordinated (e.g., $Mo_2(O_2CCH_3)_4 \cdot 2py$, $Ru_2(O_2CC_3H_7)_4Cl$). With Cr_2^{4+} axial ligands are usually present, although they can be removed without otherwise decomposing the compound, and they are held by relatively long bonds, as in $Cr_2(O_2CCH_3)_4 \cdot 2H_2O$ and $[Cr_2(CO_3)_4(H_2O)_2]^{4-}$. Nevertheless, there is a clear general trend: with strong multiple M–M bonds the capacity of the metal atoms to bind ligands along the extension of the M–M bond axis is small and often negligible. With the strongest M–M bonds their axial positions are usually vacant. While steric factors may play some role, this phenomenon seems certain to have a fundamentally electronic origin. It is also relevant that in mononuclear octahedral complexes containing a multiple metal–ligand bond, the ligand trans to this bond is usually weakly bound and is sometimes absent.

In this paper we report some work which arose out of a desire to better define and better understand this phenomenon. The experimental work began with the discovery that the reaction of the dipyrazolyldiethylborate ion, $[(C_3H_3N_2)_2(C_2H_5)_2B]^-$, with $Mo_2(O_2CCH_3)_4$ gives two products, the quantities of which depend on reactant ratios

$$Mo_2(O_2CCH_3)_4 + 4(pz)_2Et_2B^- \rightarrow Mo_2((pz)_2Et_2B)_4 + 4CH_3COO^-$$

$$Mo_2(O_2CCH_3)_4 + 2(pz)_2Et_2B^- \rightarrow Mo_2(O_2CCH_3)_2((pz)_2Et_2B)_2 + 2CH_3COO^-$$

The structure of the mixed-ligand product was determined crystallographically and found to be, as expected, symmetrical, with two bridging CH_3CO_2 groups and one bidentate $(pz)_2Et_2B$ group on each metal atom.

A consideration of this structure then led us to the following questions: What would happen if the $(pz)_2Et_2B$ groups were replaced with $(pz)_3RB$ groups, which have a strong tendency to be tridentate, occupying three mutually cis positions? Could one in this way force the Mo_2^{4+} unit to accept two moderately strong axial donor atoms? In this paper we report the experimental work which led to these questions as well as the work done to answer them, and we discuss, briefly, our views on why multiply bonded M_2 species resist the attachment of axial ligands.

Experimental Section

All manipulations were carried out under an atmosphere of dry argon. All solvents were distilled from an Na–K alloy immediately before use and transferred by syringe or degassed by alternate freezing and thawing in vacuo after being dried in molecular sieves.

Preparation of $Mo_2((pz)_2BEt_2)(OOCCH_3)_2$. $Na(pz)_2BEt_2$ (0.52 g), prepared according to the published procedure,[2] was added to a suspension of 0.50 g of $Mo_2(OOCCH_3)_4$, prepared as before,[3] in 15 ml of glyme (1,2-dimethoxyethane). After the reaction mixture had been stirred and refluxed for $^1/_2$ h, the solvent was removed by vacuum and benzene (25 ml) was added. The resulting solution was filtered, and after reduction of the volume, it was chromatographed on Florisil using benzene as eluent. Two bands were formed. The first one contained a small amount of a blue compound (see below) and the second one consisted of the red $Mo_2((pz)_2BEt_2)_2(OOCCH_3)_2$.

Preparation of $Mo_2((pz)_2BEt_2)_4$. The procedure followed was the same as before except that a small excess of ligand (1.25 g) was used. Toluene was used as solvent. Filtration of the benzene solution left a green solid and gave a solution of the blue compound, mentioned above, which was chromatographed on Florisil. The ^1H NMR spectrum had no acetate resonance and the mass spectrum showed a small parent ion peak for the formula $Mo_2((pz)_2BEt_2)_4$. We intend to describe this compound more fully in a later report.

Preparation of $Mo_2((pz)_3BH)_2(OOCCH_3)_2$. To a suspension of 0.4 g of $Mo_2(OOCCH_3)_4$ in 25 ml of glyme, 0.48 g of $KHB(pz)_3$, prepared following the published procedure,[4] was added. The mixture was stirred at room temperature for about $^1/_2$ h and the reaction mixture was then filtered. The remaining red powder was purified by extraction with glyme or toluene in a Soxhlet apparatus. The compound is virtually insoluble in most of the common solvents.

Crystal Data and Structure Determination for $Mo_2((pz)_2BEt_2)_2(OOCCH_3)_2 \cdot CS_2$. A red crystal, obtained by recrystallization from carbon disulfide, measuring about 0.50 × 0.32 × 0.40 mm was sealed in a capillary under argon and examined on a Syntex $P\bar{1}$ four-circle automatic diffractometer. Axial photographs and ω scans of several intense reflections showed that the crystal quality was good and that it was suitable for x-ray diffraction studies. At small scattering angles the peak widths at half-height were <0.2°.

For calculation of lattice parameters, 15 of the strongest reflections in the range 25° < 2θ < 32° were selected to give a variety of crystal orientations. Based on angular settings for these reflections, the refined lattice parameters obtained from the Syntex software package are (Mo Kα, λ 0.71073 Å) a = 12.933 (4) Å, b = 13.088 (4) Å, c = 11.592 (4) Å, α = 101.68 (3)°, β = 112.86 (3)°, γ = 69.69 (2)°, and V = 1690 (1) Å^3. For the triclinic space group $P\bar{1}$ with Z = 2 and mol wt 753.96, the calculated density is 1.481 g cm^{-3}.

Intensity data were collected at 23 ± 1 °C using graphite-monochromatized Mo Kα radiation and a θ–2θ scan rate varying from 4 to 24°/min, depending on the intensity of the reflection. Background measurements were made at both limits of each scan. Of the 6188 integrated intensities collected in the range 0° < 2θ (Mo Kα) < 50°,

4841 unique observations with $I > 3\sigma(I)$ were retained as observed data and corrected for Lorentz and polarization effects. Three standard reflections measured repeatedly every 100 data points showed a significant but apparently linear decomposition; the experimental structure factors were corrected for decomposition. Since the linear absorption coefficient of this compound is 8.9 cm^{-1} for Mo Kα radiation, for any reflection, the maximum relative error due to absorption is <4% F_o, and the data were not corrected for absorption.

A three-dimensional Patterson map, as expected, was dominated by Mo–Mo vectors. Analysis of the map gave the positions for both molybdenum atoms. A difference Fourier synthesis based on refined molybdenum positions revealed all the rest of the nonhydrogen atoms. All atoms were assigned isotropic thermal parameters and least-squares refinement then gave discrepancy indices

$$R_1 = \Sigma \| F_o | - | F_c \| / \Sigma | F_o | = 0.069$$

$$R_2 = [\Sigma w(|F_o| - |F_c|)^2 / \Sigma w |F_o|^2]^{1/2} = 0.107$$

Refinement was continued with anisotropic thermal parameters for the molybdenum atoms and isotropic thermal parameters for the rest of the nonhydrogen atoms to convergence at $R_1 = 0.061$, $R_2 = 0.099$; the error in an observation of unit weight was 2.7. No attempt was made to locate the hydrogen atoms. The function minimized was $\sum w(|F_o| - |F_c|)^2$ where $p = 0.06$ in the previously defined expression for the weights[5,6] and the scattering factors were from ref 7. Corrections for anomalous scattering by molybdenum and sulfur were taken from Cromer and Liberman.[8] A final difference map showed some relatively high peaks in the neighborhood of the carbon disulfide molecule. Since the crystal decomposition during data collection is almost certainly due to loss of carbon disulfide, the peaks are readily understood to reflect the inadequacy of the simple decomposition correction applied to the intensity data. Otherwise, the map was judged to be free of significant features.

An analysis of $\sum w(|F_o| - |F_c|)^2$ as a function of $|F_o|$ showed that the original choice for the p parameter used in the calculation of the standard deviation of the intensity (cf. the program DATARED[9]) was satisfactory. No unusual trends were observed in an analysis of $\sum w(|F_o| - |F_c|)^2$ as a function of reflection number, $\lambda^{-1} \sin\theta$, or various classes of indices. A list of observed and calculated structure factors is available.[10]

Data and Structure Refinement for $Mo_2((pz)_3BH)_2(OOCCH_3)_2$. A red crystal measuring about 0.2 × 0.1 × 0.1 mm obtained from the reaction flask was mounted in a sealed capillary. From ω scans and both precession and rotation photographs, it was found that the crystal was slightly fractured but of acceptable quality for data collection. Despite its imperfections, this crystal was the best one among many that were examined.

Cell constants were obtained by carefully centering 15 reflections (21 ± 1 °C) in the range $5° < 2\theta < 15°$. A least-squares refinement (Mo Kα, λ 0.71073 Å) gave a = 11.238 (8), b = 13.698 (6), c = 9.681 (7), β = 99.34 (6)°, and V = 1471 (2) Å^3. The data collection procedure was similar to that given above except that the scan rate varied from 2 to 24°/min. After correction for Lorentz and polarization effects, a correction for decomposition was applied. As before, the linear absorption coefficient is 8.9 cm^{-1} and no corrections were made for the still smaller absorption errors. Of the 2108 reflections collected in the range $0° < 2\theta(\text{Mo K}\alpha) < 45°$, 1402 unique observations with $I > 2\sigma(I)$ were retained as observed data. The systematic absences suggested the monoclinic space groups $P2_1/m$ or $P2_1$. For either one, with $Z = 2$ and a mol wt 736.03, the calculated density is 1.662 g cm^{-3}.

The positions of the molybdenum atoms were obtained from a three-dimensional Patterson map. Solution of the structure was attempted in the centrosymmetric space group $P2_1/m$. After a series of unsuccessful attempts at finding a good model, a statistical analysis of the structure amplitudes suggested that the probable space group was the polar space group $P2_1$. The process of finding a satisfactory model was slow and complicated by the initial pseudomirror containing the Mo–Mo bond. The customary heavy-atom method of structure solution[11] was not successful until entire idealized acetate groups and pyrazolyl rings were set at positions which seemed chemically reasonable using the apparent positions of two or more of their atoms in a difference Fourier synthesis. Proceeding in this way, a series of atoms gradually appeared in the difference maps, leading finally to the entire structure. The model found in this way was refined with isotropic temperature factors to discrepancy indices of $R_1 = 0.084$ and $R_2 = 0.090$. The molybdenum atoms were then assigned anisotropic thermal parameters and further least-squares refinement led to $R_1 = 0.066$ and $R_2 = 0.070$. At this point, attempts to identify the correct enantiomorph failed; refinement of the alternative model gave the same R values and virtually identical patterns of bond parameters. For that reason, refinement was continued without the imaginary component of the molybdenum atom scattering factors. At this point, there was a final question with respect to the correct identity of the atoms bonded to 5N(1). Structure refinements with averaging and permutation of the carbon and nitrogen scattering factors for the two atoms in question resulted in thermal parameter patterns that strongly supported the original choice of orientation for the pyrazolyl ring and, consequently, the identification of 5N(2) and 5C(3). No attempt was made to determine the experimental positions for the hydrogen atoms, but for the final refinement pyrazolyl-ring hydrogen atoms were included at fixed idealized positions 1.0 Å from the carbon atoms to which they are bonded.

The structure refinement converged at final R factors of 0.064 and 0.067 and an error in an observation of unit weight of 1.39. A final difference map was judged to be free of significant features. No unusual trends were observed in an analysis of $\sum w(|F_o| - |F_c|)^2$ as a function of $|F_o|$, reflection number, $\lambda^{-1} \sin\theta$, or various classes of indices. A table of observed and calculated structure factor amplitudes is available.[10]

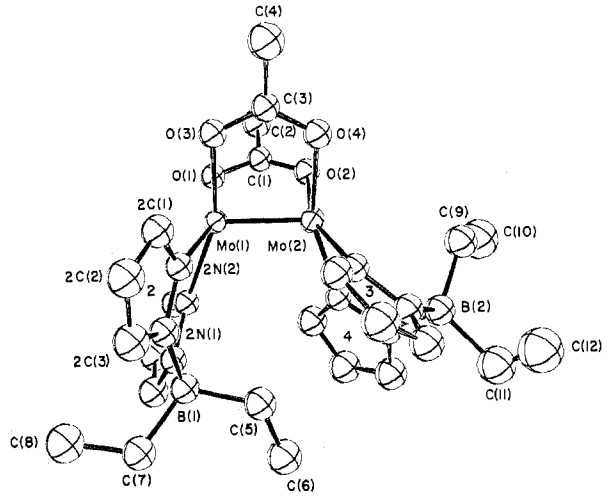

Figure 1. ORTEP view of $Mo_2((pz)_2BEt_2)_2(O_2CCH_3)_2$ showing the boat configuration of the pyrazolylborato ligands. The atom-numbering scheme used in the tables is defined. Pyrazolyl ring 1 is behind pyrazolyl ring 2. The atoms are represented by 50% probability thermal ellipsoids.

Results

For $Mo_2((pz)_2BEt_2)_2(O_2CCH_3)_2 \cdot CS_2$, the atomic positional parameters and thermal parameters are listed in Table I. The molecular structure is shown in Figure 1, which also defines the atom-numbering scheme. The interatomic distances are listed in Table II and bond angles are listed in Table III. The packing of the molecule can be seen in Figure 2 which shows a very weak interaction (3.159 Å) between Mo(1) and O(1) from an acetate group in another molecule in a different unit cell. The atomic positional parameters for $Mo_2((pz)_3BH)_2(O_2CCH_3)_2$ are listed in Table IV. The interatomic distances are given in Table V and the bond angles in Table VI. Figure 3 shows the molecular structure and defines the atom-numbering scheme. For $Mo_2((pz)_3BH)_2(O_2CCH_3)_2$ there are no contacts less than 4.5 Å between Mo(1) and atoms from neighboring molecules.

Discussion

As reported in the Experimental Section, the reaction of $Mo_2(O_2CCH_3)_4$ with $NaB(pz)_2Et_2$ yields both $Mo_2(B(pz)_2Et_2)_4$ (**1**) and $Mo_2(O_2CCH_3)_2(B(pz)_2Et_2)_2$ (**2**). Further study of the first compound is in progress and it will not be discussed here. The structure of compound **2** presents several

Table I. Positional and Thermal Parameters[a] and Their Estimated Standard Deviations for $Mo_2(Et_2B(pz)_2)_2(O_2CCH_3)_2 \cdot CS_2$

Atom	x	y	z	B_{11}	B_{22}	B_{33}	B_{12}	B_{13}	B_{23}
Mo(1)	0.107 46 (5)	−0.155 68 (5)	0.097 85 (5)	2.40 (2)	2.39 (2)	1.96 (3)	−0.75 (3)	0.58 (2)	0.26 (2)
Mo(2)	0.066 65 (5)	−0.236 77 (5)	0.208 96 (5)	2.81 (3)	2.32 (2)	2.11 (3)	−0.77 (2)	0.77 (2)	0.28 (1)

Atom	x	y	z	B_{iso}, Å^2	Atom	x	y	z	B_{iso}, Å^2
O(1)	−0.0551 (4)	−0.0317 (4)	0.0693 (4)	2.69 (8)	2C(3)	0.4567 (8)	−0.3100 (7)	0.0848 (8)	4.1 (2)
O(2)	−0.0999 (4)	−0.1200 (4)	0.1770 (5)	2.99 (9)	3C(3)	0.3435 (7)	−0.5037 (7)	0.4040 (8)	3.8 (2)
O(3)	0.0279 (4)	−0.2457 (4)	−0.0669 (5)	2.85 (8)	4C(3)	0.2100 (8)	−0.1701 (7)	0.6078 (9)	4.4 (2)
O(4)	−0.0092 (4)	−0.3317 (4)	0.0504 (5)	3.04 (9)	B(1)	0.4205 (7)	−0.1829 (7)	0.2794 (8)	3.1 (1)
1N(1)	0.3225 (5)	−0.0664 (5)	0.2759 (5)	2.8 (1)	B(2)	0.1770 (8)	−0.3543 (8)	0.4803 (9)	3.4 (2)
2N(1)	0.3816 (5)	−0.2439 (5)	0.1444 (6)	2.9 (1)	C(1)	−0.1280 (6)	−0.0447 (6)	0.1105 (7)	2.8 (1)
3N(1)	0.2466 (5)	−0.4145 (5)	0.3879 (6)	3.1 (1)	C(2)	−0.2523 (7)	0.0329 (7)	0.0729 (8)	4.1 (2)
4N(1)	0.1787 (5)	−0.2337 (5)	0.4981 (6)	3.2 (1)	C(3)	−0.0117 (6)	−0.3173 (6)	−0.0548 (7)	2.9 (1)
1N(2)	0.2028 (5)	−0.0455 (5)	0.2201 (5)	2.6 (1)	C(4)	−0.0627 (8)	−0.3845 (8)	−0.1674 (9)	4.5 (2)
2N(2)	0.2731 (5)	−0.2512 (5)	0.0726 (5)	2.6 (1)	C(5)	0.4211 (7)	−0.2517 (7)	0.3804 (8)	3.7 (1)
3N(2)	0.2087 (5)	−0.3839 (5)	0.2681 (5)	2.7 (1)	C(6)	0.4645 (8)	−0.2092 (8)	0.5186 (9)	4.4 (2)
4N(2)	0.1269 (5)	−0.1694 (5)	0.4008 (6)	2.8 (1)	C(7)	0.5464 (7)	−0.1649 (7)	0.3095 (8)	3.9 (2)
1C(1)	0.1541 (6)	0.0607 (6)	0.2462 (7)	3.2 (1)	C(8)	0.5540 (9)	−0.0972 (8)	0.2180 (9)	5.3 (2)
2C(1)	0.2807 (7)	−0.3202 (6)	−0.0292 (7)	3.3 (1)	C(9)	0.0434 (8)	−0.3587 (7)	0.4160 (8)	4.1 (2)
3C(1)	0.2818 (7)	−0.4534 (6)	0.2116 (7)	3.3 (1)	C(10)	−0.0394 (11)	−0.2840 (11)	0.4895 (12)	6.7 (3)
4C(1)	0.1273 (7)	−0.0652 (7)	0.4492 (8)	3.9 (1)	C(11)	0.2506 (9)	−0.4076 (9)	0.6172 (10)	5.3 (2)
1C(2)	0.2376 (8)	0.1099 (7)	0.3182 (9)	4.3 (2)	C(12)	0.2365 (11)	−0.4808 (11)	0.6180 (12)	7.1 (3)
2C(2)	0.3968 (8)	−0.3592 (7)	−0.0228 (9)	4.3 (2)	C(S)	0.2902 (11)	0.2875 (11)	−0.0054 (12)	6.6 (3)
3C(2)	0.3676 (8)	−0.5298 (8)	0.2919 (9)	4.4 (2)	S(1)	0.2334 (3)	0.3597 (3)	−0.1014 (4)	8.1 (1)
4C(2)	0.1773 (8)	−0.0634 (8)	0.5803 (9)	4.7 (2)	S(2)	0.3613 (5)	0.2054 (5)	0.1020 (6)	11.8 (1)
1C(3)	0.3461 (7)	0.0262 (7)	0.3352 (8)	3.8 (2)					

[a] The B_{ij} (in Å^2) Are related to the dimensionless β_{ij} employed during refinement as $B_{ij} = 4\beta_{ij}/a^*_i a^*_j$.

Table II. Interatomic Distances (A°)[a-c] for $Mo_2(Et_2B(pz)_2)_2(O_2CCH_3)_2 \cdot CS_2$

Mo(1)-Mo(2)	2.129 (1)	B(1)-1N(1)	1.60 (1)
Mo(1)-O(1)	2.116 (5)	B(1)-2N(1)	1.58 (1)
Mo(1)-O(3)	2.120 (5)	B(1)-C(5)	1.61 (1)
Mo(1)-1N(2)	2.158 (6)	B(1)-C(7)	1.62 (1)
Mo(1)-2N(2)	2.172 (6)	B(2)-3N(1)	1.58 (1)
Mo(2)-O(2)	2.106 (5)	B(2)-4N(1)	1.56 (1)
Mo(2)-O(4)	2.099 (5)	B(2)-C(9)	1.61 (1)
Mo(2)-3N(2)	2.158 (6)	B(2)-C(11)	1.65 (1)
Mo(2)-4N(2)	2.161 (6)	C(5)-C(6)	1.53 (1)
C(1)-O(1)	1.280 (8)	C(7)-C(8)	1.56 (1)
C(1)-O(2)	1.240 (8)	C(9)-C(10)	1.57 (1)
C(1)-C(2)	1.520 (11)	C(11)-C(12)	1.54 (1)
C(3)-O(3)	1.267 (9)	C(S)-S(1)	1.41 (1)
C(3)-O(4)	1.259 (9)	C(S)-S(2)	1.58 (1)
C(3)-C(4)	1.477 (11)	Mo(1)-B(1)	3.692 (9)
		Mo(2)-B(2)	3.353 (9)

Pyrazolyl Rings

	Ring 1	Ring 2	Ring 3	Ring 4
N(1)-N(2)	1.375 (8)	1.351 (8)	1.375 (8)	1.354 (8)
N(2)-C(1)	1.338 (9)	1.346 (9)	1.339 (9)	1.36 (1)
C(1)-C(2)	1.36 (1)	1.38 (1)	1.38 (1)	1.40 (1)
C(2)-C(3)	1.42 (1)	1.36 (1)	1.40 (1)	1.38 (1)
C(3)-N(1)	1.34 (1)	1.36 (1)	1.36 (1)	1.37 (1)

[a] Here and in other tables numbers in parentheses are the estimated standard deviations in the last significant digits. [b] Atoms are labeled as in Figure 1. [c] Rings 1-4 are identified in Figure 1.

Table III. Bond Angles (deg) for $Mo_2(Et_2B(pz)_2)_2(O_2CCH_3)_2 \cdot CS_2$

Mo(2)-Mo(1)-O(1)	90.9 (1)	Mo(2)-4N(2)-4C(1)	130.9 (5)
Mo(2)-Mo(1)-O(3)	90.7 (1)	Mo(1)-O(1)-C(1)	117.3 (4)
Mo(2)-Mo(1)-1N(2)	108.7 (2)	O(1)-C(1)-C(2)	118.2 (6)
Mo(2)-Mo(1)-2N(2)	110.4 (2)	O(1)-C(1)-O(2)	121.6 (6)
O(1)-Mo(1)-1N(2)	91.7 (2)	O(2)-C(1)-C(2)	120.1 (6)
O(1)-Mo(1)-2N(2)	158.3 (2)	Mo(2)-O(2)-C(1)	118.8 (5)
O(1)-Mo(1)-O(3)	89.7 (2)	Mo(1)-O(3)-C(3)	117.9 (5)
O(3)-Mo(1)-1N(2)	160.6 (2)	O(3)-C(3)-C(4)	119.0 (7)
O(3)-Mo(1)-2N(2)	86.0 (2)	O(3)-C(3)-O(4)	121.5 (7)
1N(2)-Mo(1)-2N(2)	85.5 (2)	O(4)-C(3)-C(4)	119.6 (7)
Mo(1)-Mo(2)-O(2)	91.0 (1)	Mo(2)-O(4)-C(3)	118.6 (5)
Mo(1)-Mo(2)-O(4)	91.3 (1)	1N(1)-B(1)-2N(1)	106.8 (6)
Mo(1)-Mo(2)-3N(2)	109.1 (2)	1N(1)-B(1)-C(5)	108.6 (6)
Mo(1)-Mo(2)-4N(2)	107.5 (2)	1N(1)-B(1)-C(7)	109.6 (6)
O(2)-Mo(2)-3N(2)	159.6 (2)	2N(1)-B(1)-C(5)	108.9 (6)
O(2)-Mo(2)-4N(2)	90.6 (2)	2N(1)-B(1)-C(7)	109.5 (6)
O(2)-Mo(2)-O(4)	88.7 (2)	C(5)-B(1)-C(7)	113.3 (7)
O(4)-Mo(2)-3N(2)	87.2 (2)	B(1)-C(5)-C(6)	116.6 (7)
O(4)-Mo(2)-4N(2)	161.2 (2)	B(1)-C(7)-C(8)	117.1 (7)
3N(2)-Mo(2)-4N(2)	86.9 (2)	3N(1)-B(2)-4N(1)	105.2 (6)
Mo(1)-1N(2)-1N(1)	127.7 (4)	3N(1)-B(2)-C(9)	109.5 (7)
Mo(1)-1N(2)-1C(1)	124.9 (5)	3N(1)-B(2)-C(11)	108.5 (7)
Mo(1)-2N(2)-2N(1)	127.6 (4)	4N(1)-B(2)-C(9)	109.7 (7)
Mo(1)-2N(2)-2C(1)	123.4 (5)	4N(1)-B(2)-C(11)	108.2 (7)
Mo(2)-3N(2)-3N(1)	120.8 (4)	C(9)-B(2)-C(11)	115.2 (7)
Mo(2)-3N(2)-3C(1)	131.5 (5)	B(2)-C(9)-C(10)	113.5 (8)
Mo(2)-4N(2)-4N(1)	121.4 (5)	B(2)-C(11)-C(12)	113.3 (9)

Pyrazolyl Rings

	Ring 1	Ring 2	Ring 3	Ring 4
N(1)-N(2)-C(1)	107.1 (6)	108.6 (6)	107.4 (6)	107.6 (6)
N(2)-C(1)-C(2)	111.0 (7)	109.1 (7)	110.6 (7)	109.2 (8)
C(1)-C(2)-C(3)	105.0 (7)	105.3 (8)	105.4 (8)	105.4 (8)
C(2)-C(3)-N(1)	107.9 (7)	110.0 (8)	107.9 (7)	109.0 (8)
C(3)-N(1)-N(2)	108.9 (6)	107.0 (6)	108.7 (6)	108.8 (6)

features of interest, which we shall now discuss.

The Mo–Mo distance in **2**, namely, 2.129 (1) Å, is significantly greater than the Mo–Mo distances in tetracarboxylato species, which are 2.093 (2) Å for $Mo_2(O_2CCH_3)_4$,[12] 2.090 (4) Å for $Mo_2(O_2CCF_3)_4$,[13] 2.091 (2) Å for $Mo_2(O_2CH)_4$,[14] and 2.115 (1) Å for $Mo_2(O_2CCH_2NH_2)_4(SO_4)_2 \cdot 2H_2O$.[15] This lengthening probably has two causes. First, the π orbitals of bridging carboxylato groups appear to become extensively involved in the metal–metal bonding,[16] probably in such a way as to strengthen it. Half of this contribution is lost in **2**. Second, repulsive forces between the bulky $B(pz)_2Et_2^-$ ligands may be expected to stretch the bond. Another structural feature that is most likely due to these nonbonded repulsions is the large values of the Mo–Mo–N angles, which run 107.5–110.4°, whereas in $Mo_2Cl_8^{4-}$ the analogous Mo–Mo–Cl angles are about 104°. From this line of reasoning, we would expect an even longer Mo–Mo bond in **1**. It is even possible that as the ligand–ligand repulsive forces increase and the δ–δ interaction becomes weaker because of the increasing Mo–Mo distance, there may be some twisting of the eclipsed rotational configuration. We hope to determine the structure of **1** in order to check these points.

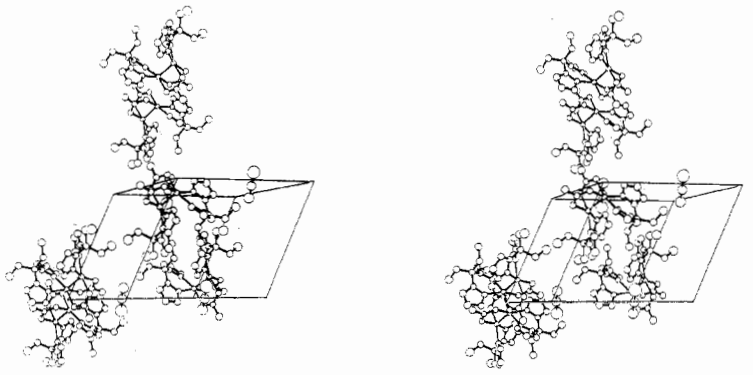

Figure 2. Stereoscopic view of the structure of $Mo_2((pz)_2BEt_2)_2(O_2CCH_3)_2 \cdot CS_2$ showing the crystal packing. The *a* axis points into the paper, the *b* axis is horizontal, and the *c* axis is vertical. The atoms are represented by 50% probability thermal ellipsoids.

Table IV. Positional and Thermal Parameters[a] and Their Estimated Standard Deviations for $Mo_2((pz)_3BH)_2(O_2CCH_3)_2$

Atom	*x*	*y*	*z*	B_{11}	B_{22}	B_{33}	B_{12}	B_{13}	B_{23}
Mo(1)	−0.3208 (1)	−0.2596 (3)	−0.0919 (2)	2.59 (6)	3.73 (7)	3.23 (9)	0.9 (1)	1.2 (8)	0.6 (1)
Mo(2)	−0.1445 (1)	−0.25	−0.1496 (2)	2.08 (5)	2.7 (1)	3.30 (6)	−0.05 (12)	0.87 (6)	−0.07 (12)
Atom	*x*	*y*	*z*	B_{iso}, Å^2	Atom	*x*	*y*	*z*	B_{iso}, Å^2
O(1)	−0.278 (1)	−0.388 (1)	0.020 (2)	3.7 (3)	5C(1)	−0.687 (3)	−0.175 (2)	−0.728 (3)	5.5 (7)
O(2)	−0.098 (1)	−0.385 (1)	−0.046 (2)	3.6 (3)	6C(1)	0.172 (2)	−0.280 (2)	−0.106 (2)	2.9 (5)
O(3)	−0.268 (1)	−0.169 (1)	0.087 (2)	4.3 (4)	1C(2)	−0.562 (3)	−0.455 (2)	−0.359 (3)	4.5 (7)
O(4)	−0.085 (1)	−0.166 (1)	0.031 (2)	3.7 (3)	2C(2)	−0.532 (2)	0.002 (2)	−0.214 (3)	4.3 (6)
1N(1)	−0.486 (2)	−0.309 (1)	−0.376 (2)	2.6 (4)	3C(2)	−0.154 (2)	0.039 (2)	−0.343 (2)	3.5 (5)
2N(1)	−0.475 (1)	−0.129 (1)	−0.324 (2)	2.5 (3)	4C(2)	−0.198 (2)	−0.413 (2)	−0.548 (3)	4.8 (6)
3N(1)	−0.081 (2)	−0.107 (1)	−0.371 (2)	2.8 (4)	5C(2)	−0.594 (3)	−0.196 (2)	−0.796 (3)	5.5 (6)
4N(1)	−0.100 (1)	−0.278 (1)	−0.451 (2)	3.2 (4)	6C(2)	0.264 (2)	−0.268 (2)	−0.185 (2)	4.5 (5)
5N(1)	−0.527 (2)	−0.192 (1)	−0.571 (2)	3.0 (4)	1C(3)	−0.562 (2)	−0.377 (2)	−0.442 (3)	3.9 (5)
6N(1)	0.090 (1)	−0.224 (1)	−0.308 (2)	3.0 (4)	2C(3)	−0.536 (2)	−0.047 (2)	−0.338 (3)	3.0 (6)
1N(2)	−0.436 (2)	−0.343 (1)	−0.252 (2)	3.1 (4)	3C(3)	−0.090 (2)	−0.017 (2)	−0.420 (3)	4.3 (6)
2N(2)	−0.425 (2)	−0.141 (1)	−0.188 (2)	2.5 (4)	4C(3)	−0.126 (2)	−0.331 (2)	−0.573 (3)	4.4 (6)
3N(2)	−0.146 (2)	−0.112 (1)	−0.265 (2)	3.3 (4)	5C(3)	−0.496 (2)	−0.204 (2)	−0.702 (2)	3.7 (5)
4N(2)	−0.158 (2)	−0.323 (1)	−0.350 (2)	3.1 (4)	6C(3)	0.215 (2)	−0.236 (2)	−0.302 (2)	3.7 (5)
5N(2)	−0.648 (2)	−0.177 (2)	−0.592 (2)	4.0 (4)	B(1)	−0.447 (2)	−0.212 (2)	−0.429 (3)	2.5 (5)
6N(2)	0.068 (1)	−0.255 (2)	−0.178 (2)	3.4 (4)	B(2)	−0.011 (2)	−0.193 (2)	−0.422 (3)	2.4 (5)
1C(1)	−0.481 (2)	−0.431 (2)	−0.239 (3)	4.0 (5)	C(1)	−0.178 (2)	−0.431 (2)	0.017 (2)	3.1 (4)
2C(1)	−0.460 (2)	−0.061 (2)	−0.126 (2)	3.3 (5)	C(2)	−0.144 (2)	−0.522 (2)	0.085 (3)	4.7 (6)
3C(1)	−0.187 (2)	−0.025 (2)	−0.248 (2)	4.0 (5)	C(3)	−0.165 (2)	−0.138 (2)	0.107 (3)	4.0 (5)
4C(1)	−0.213 (2)	−0.400 (2)	−0.409 (2)	3.6 (5)	C(4)	−0.123 (3)	−0.059 (2)	0.214 (3)	6.1 (7)

[a] The B_{ij} (Å^2) are related to the dimensionless β_{ij} employed during refinement as $B_{ij} = 4\beta_{ij}/a^*_i a^*_j$.

Table V. Interatomic Distances (Å)[a,b] for $Mo_2((pz)_3BH)_2(O_2CCH_3)_2$

Mo(1)-Mo(2)	2.147 (3)	C(1)-C(2)	1.44 (3)
Mo(1)-O(1)	2.08 (2)	C(3)-O(3)	1.22 (3)
Mo(1)-O(3)	2.13 (2)	C(3)-O(4)	1.30 (3)
Mo(1)-1N(2)	2.18 (2)	C(3)-C(4)	1.52 (4)
Mo(1)-2N(2)	2.13 (2)	B(1)-1N(1)	1.52 (3)
Mo(2)-O(2)	2.13 (2)	B(1)-2N(1)	1.59 (3)
Mo(2)-O(4)	2.11 (2)	B(1)-5N(1)	1.54 (3)
Mo(2)-3N(2)	2.19 (2)	B(2)-3N(1)	1.54 (3)
Mo(2)-4N(2)	2.16 (2)	B(2)-4N(1)	1.53 (3)
Mo(2)-6N(2)	2.45 (1)	B(2)-6N(1)	1.51 (3)
C(1)-O(1)	1.28 (2)	Mo(1)-B(1)	3.41 (3)
C(1)-O(2)	1.32 (2)	Mo(2)-B(2)	3.33 (2)

Pyrazolyl Rings

	Ring 1	Ring 2	Ring 3	Ring 4	Ring 5	Ring 6
N(1)-N(2)	1.32 (2)	1.36 (2)	1.36 (2)	1.41 (2)	1.36 (2)	1.39 (2)
N(2)-C(1)	1.31 (3)	1.34 (3)	1.30 (3)	1.31 (3)	1.32 (3)	1.31 (2)
C(1)-C(2)	1.40 (4)	1.38 (3)	1.37 (3)	1.39 (3)	1.36 (3)	1.40 (3)
C(2)-C(3)	1.34 (3)	1.37 (3)	1.36 (3)	1.43 (3)	1.31 (3)	1.26 (3)
C(3)-N(1)	1.34 (3)	1.32 (3)	1.31 (3)	1.37 (3)	1.38 (3)	1.40 (2)

[a] Atoms are labeled as in Figure 3. [b] Rings 1-6 are identified in Figure 3.

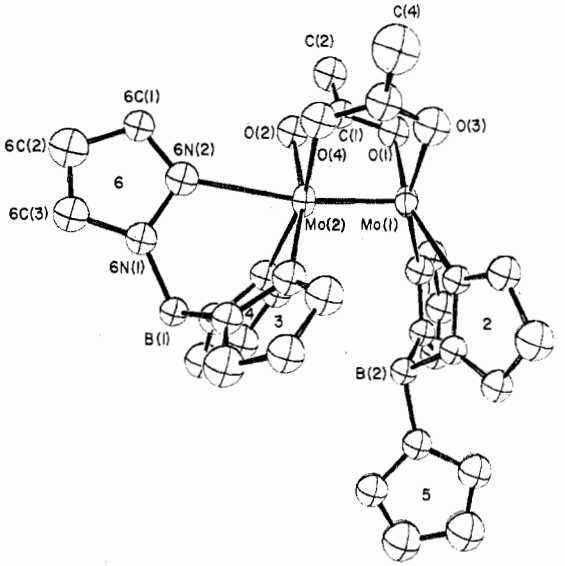

Figure 3. ORTEP view of the $Mo_2((pz)_3BH)_2(O_2CCH_3)_2$ molecule. The atom-numbering scheme used in the tables is defined. The atoms are represented by 50% probability thermal ellipsoids.

Another aspect of the structure of **2** has to do with interactions of donor atoms in the axial positions with the Mo atoms. In the case of all $Mo_2(O_2CR)_4$ compounds[12-15] there have been intermolecular interactions of an oxygen atom of one molecule with a Mo atom of an adjacent molecule in such a way as to give infinite chains in which both Mo atoms of

Table VI. Bond Angles (deg) for $Mo_2((pz)_3BH)_2(O_2CCH_3)_2$

Mo(2)-Mo(1)-O(1)	92.5 (4)	Mo(1)-1N(2)-1C(1)	127 (2)
Mo(2)-Mo(1)-O(3)	91.6 (5)	Mo(1)-2N(2)-2N(1)	129 (1)
Mo(2)-Mo(1)-1N(2)	108.5 (5)	Mo(1)-2N(2)-2C(1)	128 (1)
Mo(2)-Mo(1)-2N(2)	107.8 (5)	Mo(2)-3N(2)-3N(1)	118 (1)
O(1)-Mo(1)-1N(2)	89.2 (7)	Mo(2)-3N(2)-3C(1)	134 (2)
O(1)-Mo(1)-2N(2)	159.7 (6)	Mo(2)-4N(2)-4N(1)	117 (1)
O(1)-Mo(1)-O(3)	93.3 (7)	Mo(2)-4N(2)-4C(1)	136 (2)
O(3)-Mo(1)-1N(2)	159.7 (7)	Mo(2)-6N(2)-6N(1)	115 (1)
O(3)-Mo(1)-2N(2)	88.3 (7)	Mo(2)-6N(2)-6C(1)	138 (1)
1N(2)-Mo(1)-2N(2)	82.6 (8)	Mo(1)-O(1)-C(1)	120 (1)
Mo(1)-Mo(2)-O(2)	89.3 (4)	O(1)-C(1)-C(2)	124 (2)
Mo(1)-Mo(2)-O(4)	89.9 (4)	O(1)-C(1)-O(2)	117 (2)
Mo(1)-Mo(2)-3N(2)	104.7 (5)	O(2)-C(1)-C(2)	119 (2)
Mo(1)-Mo(2)-4N(2)	105.6 (5)	Mo(2)-O(2)-C(1)	120 (1)
Mo(1)-Mo(2)-6N(2)	170.1 (5)	Mo(1)-O(3)-C(3)	118 (2)
O(2)-Mo(2)-3N(2)	166.0 (6)	O(3)-C(3)-C(4)	123 (2)
O(2)-Mo(2)-4N(2)	90.0 (7)	O(3)-C(3)-O(4)	122 (2)
O(2)-Mo(2)-6N(2)	81.8 (8)	O(4)-C(3)-C(4)	115 (2)
O(2)-Mo(2)-O(4)	93.7 (7)	Mo(2)-O(4)-C(3)	118 (1)
O(4)-Mo(2)-3N(2)	85.8 (7)	1N(1)-B(1)-2N(1)	108 (2)
O(4)-Mo(2)-4N(2)	164.1 (7)	1N(1)-B(1)-5N(1)	107 (2)
O(4)-Mo(2)-6N(2)	85.8 (7)	2N(1)-B(1)-5N(1)	107 (2)
3N(2)-Mo(2)-4N(2)	86.9 (8)	3N(1)-B(2)-4N(1)	107 (2)
3N(2)-Mo(2)-6N(2)	83.9 (8)	3N(1)-B(2)-6N(1)	110 (2)
4N(2)-Mo(2)-6N(2)	79.4 (7)	4N(1)-B(2)-6N(1)	108 (2)
Mo(1)-1N(2)-1N(1)	125 (1)		

Pyrazolyl Rings

	Ring 1	Ring 2	Ring 3	Ring 4	Ring 5	Ring 6
N(1)-N(2)-C(1)	107 (2)	104 (2)	107 (2)	106 (2)	108 (2)	107 (2)
N(2)-C(1)-C(2)	110 (2)	115 (2)	111 (2)	113 (2)	109 (2)	111 (2)
C(1)-C(2)-C(3)	104 (3)	100 (2)	103 (2)	103 (2)	108 (3)	106 (2)
C(2)-C(3)-N(1)	110 (2)	112 (2)	110 (2)	108 (2)	108 (2)	112 (2)
C(3)-N(1)-N(2)	109 (2)	109 (2)	108 (2)	108 (2)	106 (2)	105 (2)

each molecule experienced identical, weak coordination, with O···Mo distances in the range 2.65–2.75 Å. Because of the steric demands of the $B(pz)_2Et_2^-$ ligands, such an arrangement is impossible here; both Mo atoms cannot simultaneously be accessible to neighboring oxygen atoms. The packing arrangement does incorporate one such intermolecular contact, involving Mo(1), as can be seen in Figure 2, but it is very long, 3.16 Å, and probably has negligible influence on the Mo–Mo bond.

At Mo(2) we have an unusual arrangement. There appears to be a weak interaction between Mo(2) and an aliphatic hydrogen atom, similar to the H···Mo interactions previously observed in the electron-deficient molecules $(\eta^3\text{-}CH_2CPhCH_2)(CO)_2(B(pz)_2Et_2)Mo$[17] and $(\eta^3\text{-}C_7H_7)(CO)_2(B(pz)_2Et_2)Mo$.[18] The Mo(2)–C(9) distance is 3.293 (9) Å. If the positions of the methylene hydrogen atoms are calculated assuming approximately tetrahedral angles at C(9) and C–H distances of 1.0 Å, it turns out that there is an Mo···H distance of 2.49 Å. The electronic character of this interaction is uncertain, but the relatively short distance suggests that there is some attractive force, perhaps because of at least incipient formation of a three-center, two-electron Mo···H–C bonding orbital as in the compounds mentioned earlier.[17,18]

We turn now to compound **3**, which, as noted in the Introduction, was prepared and studied specifically to see if the marked tendency of $B(pz)_3R^-$ ligands to form three mutually cis donor bonds of similar lengths to a metal atom[19] might not enforce the formation of two axial bonds stronger than any previously observed. In fact, the only previous example is $Mo_2(O_2CCF_3)_4\cdot 2py$[20] in which the Mo–N bonds are weak, with lengths of 2.55 Å, although even these relatively weak interactions cause a distinct increase in the Mo–Mo distance from 2.090 to 2.129 Å.

Compound **3** does not, as we had hoped, have two strong, axial donor bonds. On the contrary it has only one axial bond, and this is far longer (2.45 Å) than the other four Mo–N bonds (average 2.16 Å), though it is about 0.10 Å shorter than the Mo–N bonds in $Mo_2(O_2CCF_3)_4\cdot 2py$. Compound **3** evades the formation of any axial bond to Mo(1) by having a conformation in the chelate ring which places the third pyrazolyl ring far from the metal atom. However, once this orientation has been adopted by one tripyrazolylborate ligand, the other one is forced to take a conformation that tends to direct its third pyrazolyl group toward the axial coordination site of Mo(2), and a weak N→Mo donor bond is formed.

It is clear that the formation of axial donor bonds is unfavorable in this molecule. Steric and conformational factors would allow the approach of pyrazolyl nitrogen atoms at both axial sites simultaneously. At one end of the molecule this result is avoided by the adoption of an unsuitable ring conformation. It seems plausible to suppose that the only reason the same thing does not occur at the other end as well is that the two unsuitable conformations are mutually exclusive. Once such a conformation has been adopted at one end, there is no room for the other end to do the same. In other words, we believe that the structure suggests that if it were possible, the molecule would not have a donor bond at either end.

In view of the present as well as prior structural evidence, it is abundantly clear that for electronic reasons (apart from any steric ones which might also exist) quadruply bonded pairs of metal atoms generally have little tendency to bind electron donors in the coaxial positions. We wish to suggest a way in which this can be understood. It should be noted that the main ideas involved would apply also to the well-known fact that in mononuclear octahedral complexes the bonds trans to a multiple metal–ligand bond (M=O, M≡N) are always abnormally long and presumably weak, and, not infrequently, such trans ligands are absent.

For an axially placed donor to form a σ bond to the metal atom it is necessary for a stable, empty σ orbital to be available on the metal atom in the appropriate region of space. Such an orbital can have its provenance only in the metal d_{z^2}, s, or p_z orbitals. It was originally proposed,[21] and recent SCF–

$X\alpha$–SW calculations confirm,[16,22,23] that the d_{z^2} orbital becomes heavily involved in the M–M bond. The recent calculations also show that the valence-shell s and p orbitals are so high in energy that they make no significant contribution to any low-energy molecular orbitals. Apparently, then, there is no suitable empty σ-receptor orbital. The s and p_z orbitals are so high in energy that they cannot interact effectively with the stable lone-pair orbital of the potential donor atom and the d_{z^2} orbital contributes mainly to the M–M σ-bonding orbital which is filled and to the corresponding σ^* orbital which is empty but has a high energy.

To the extent that donors do form bonds in the axial position, they will tend to populate the σ^* orbital and thus tend to weaken the M–M σ bond. This in turn will weaken the π and δ bonds since the $d\pi$ and $d\delta$ overlaps, especially the latter, diminish more rapidly with distance than does the $d\sigma$–$d\sigma$ overlap. Thus, a crucial factor in opposing the formation of an axial donor bond is that not only would a certain amount of M–M σ-bond energy be lost, but this would lead to substantial losses of M–M π-bond and δ-bond energy. Even if the σ-bond situation by itself might be favorable, sizable losses in the other components of the M–M multiple bond due to their marked sensitivity to M–M distance will not energetically permit any significant relocation of the $d\sigma$ orbital from M–M bonding to M←L_{ax} bonding. Even in the very weak M←L_{ax} bonds that have been observed, we find that M–M bonds have increased in length by around 0.03–0.04 Å. Presumably this is all that can be tolerated before the $d\pi$–$d\pi$ and $d\delta$–$d\delta$ overlaps begin to fall too much.

Note Added in Proof. Since this paper was submitted, our efforts to obtain useful crystals of **1** have been unsuccessful. We are discontinuing this work; no further studies of **1** are currently planned.

Acknowledgment. We are grateful to the National Science Foundation for the support of this investigation through Grant No. MPS72-04536-A03.

Registry No. **1**, 59413-59-1; **2**·CS_2, 59389-00-3; **3**, 59389-01-4; $Mo_2(O_2CCH_3)_4$, 14221-06-8.

Supplementary Material Available: Listings of structure factor amplitudes (43 pages). Ordering information is given on any current masthead page.

References and Notes

(1) F. A. Cotton, *Chem. Soc. Rev.*, **4**, 27 (1975), and references therein.
(2) S. Trofimenko, *J. Am. Chem. Soc.*, **89**, 6288 (1967).
(3) A. B. Brignole and F. A. Cotton, *Inorg. Synth.*, **13**, 87 (1972).
(4) S. Trofimenko, *J. Am. Chem. Soc.*, **89**, 3170 (1967).
(5) R. D. Adams, D. M. Collins, and F. A. Cotton, *J. Am. Chem. Soc.*, **96**, 749 (1974).
(6) F. A. Cotton, B. A. Frenz, G. Deganello, and A. Shaver, *J. Organomet. Chem.*, **50**, 227 (1973).
(7) "International Tables for X-Ray Crystallography", Vol. IV, Kynoch Press, Birmingham, England, 1974.
(8) D. T. Cromer and D. Liberman, *J. Chem. Phys.*, **53**, 1891 (1970).
(9) The calculations were carried out using the following programs: DATARED, a data reduction program by Frenz; FOURIER, a Fourier summation program (based on Zalkin's FORDAP) by Dellaca and Robinson, modified by Hodgson; FAME, a program for calculating normalized structure factors by Dewar; HYDROGEN, a program for calculating atom positions in certain arrangements by Frenz and Stanislowski; NUCLS, a full-matrix least-squares program by Ibers and Doedens, similar to Busing and Levy's ORFLS; SADIAN, a distances and angles program by Baur, rewritten by Frenz; ORFFE, a function and error program by Busing, Martin, and Levy as modified by Brown, Johnson, and Theissen; ORTEP, a plotting program by Johnson; LIST, a program for listing the data by Snyder.
(10) Supplementary material.
(11) G. H. Stout and L. H. Jensen, "X-Ray Structure Determination", Macmillan, New York, N.Y., 1972.
(12) F. A. Cotton, Z. C. Mester, and T. R. Webb, *Acta Crystallogr., Sect. B*, **30**, 2768 (1974).
(13) F. A. Cotton and J. G. Norman, Jr., *J. Coord. Chem.*, **1**, 161 (1971).
(14) F. A. Cotton, J. G. Norman, Jr., B. R. Stults, and T. R. Webb, *J. Coord. Chem.*, in press.
(15) F. A. Cotton and T. R. Webb, *Inorg. Chem.*, **15**, 68 (1976).
(16) J. G. Norman, Jr., and H. J. Kolari, *J. Chem. Soc., Chem. Commun.*, 649 (1975), and private communications from J. G. Norman, Jr.
(17) F. A. Cotton, T. LaCour, and A. G. Stanislowski, *J. Am. Chem. Soc.*, **96**, 754 (1974); F. A. Cotton and A. G. Stanislowski, *ibid.*, **96**, 5074 (1974).
(18) F. A. Cotton and V. W. Day, *J. Chem. Soc., Chem. Commun.*, 416 (1974).
(19) Recent examples are found in the following references: (a) G. Avitabile, P. Ganis, and M. Nemeroff, *Acta Crystallogr., Sect. B*, **27**, 725 (1971); (b) C. S. Arcus, J. L. Wilkinson, C. Mealli, T. J. Marks, and J. A. Ibers, *J. Am. Chem. Soc.*, **96**, 7564 (1974); (c) R. J. Restivo, G. Ferguson, D. J. O'Sullivan, and F. J. Lalor, *Inorg. Chem.*, **14**, 3046 (1975).
(20) F. A. Cotton and J. G. Norman, Jr., *J. Am. Chem. Soc.*, **94**, 5697 (1972).
(21) F. A. Cotton, *Inorg. Chem.*, **4**, 334 (1965).
(22) J. G. Norman, Jr., and H. J. Kolari, *J. Am. Chem. Soc.*, **97**, 33 (1975).
(23) A. P. Mortola, J. W. Moskowitz, and N. Rosch, *Int. J. Quantum Chem. Symp.*, **No. 8**, 161–167 (1974).

Contribution from the Department of Chemistry, Texas A&M University, College Station, Texas 77843

The Scrambling of Carbonyl Groups in Guaiazulenehexacarbonyldimolybdenum and Two Isomeric Triethylphosphine Substitution Products

F. ALBERT COTTON,* PASCUAL LAHUERTA, and B. RAY STULTS

Received March 8, 1976 AIC601784

Two isomeric compounds with the formula (guaiazulene)$Mo_2(CO)_5(PEt_3)$ have been prepared and identified structurally by means of x-ray crystallography. They differ in the location of the PEt_3 group, which is on a different molybdenum atom in each case. The carbon-13 NMR spectra of both derivatives have been studied from the slow- to the fast-exchange limits. From the entire pattern of chemical shift changes which occur it has been possible to deduce for the parent hexacarbonyl (**1**) that it is the $Mo(CO)_3$ group bonded to the cyclopentadienyl group that executes internal scrambling of its CO groups more rapidly. The structure of the isomer (**2**) with the PEt_3 group attached to the molybdenum atom that is bound to the five-membered ring was refined isotropically to convergence (R_1 = 0.071, R_2 = 0.099). The crystals belong to the monoclinic system, space group $P2_1/a$, with a = 14.379 (11) Å, b = 14.569 (7) Å, c = 13.034 (6) Å, β = 94.67 (5)°. The PEt_3 group is found along the extension of the Mo–Mo bond. The structure of the isomer (**3**) was refined with anisotropic temperature parameters for the two molybdenum atoms and the phosphorus atom and isotropic temperature parameters for all other atoms to final residuals of 0.111 and 0.155. The crystals contain a disordered molecule of CH_2Cl_2 which we have not fully defined, thus accounting for the relatively high R values even though the molecular structure parameters have acceptable accuracy. The crystals belong to the space group $P2_1/c$ with a = 16.151 (10) Å, b = 12.336 (8) Å, c = 15.558 (9) Å, β = 104.27 (6)°, and V = 3004 (4) Å^3.

We have previously reported[1] that in the guaiazulenehexacarbonyldimolybdenum complex, **1**, there is a local scrambling process in each of the $Mo(CO)_3$ groups, but no general or intermetal scrambling up to the temperature range